Modeling of VHF Current Conversion from Excited Antenna Mode to Differential Mode at Transmission Line Terminals

Mohammad Heggo, *Student Member, IEEE*, Xu Zhu, *Senior Member, IEEE*, Yi Huang, *Senior Member, IEEE* and Sumei Sun, *Fellow, IEEE*

***Abstract*—The current induced by incident electric field can convert from antenna mode to differential mode at unbalanced terminals of transmission lines (TLs), causing severe interference to a number of applications such as broadband power line communication, especially in the very high frequency (VHF) band. The previous work on modeling the current conversion is not applicable to VHF. We present a new model of the VHF current conversion which includes a general formula for the antenna mode characteristic impedance and two solutions to the formulated problem: a) a numerical solution referred to as the antenna theory numerical (ATN) approach, which gives the exact value of the characteristic impedance; b) an analytical solution referred to as the enhanced TL approximation (ETLA) approach, which gives the mean of the characteristic impedance. This is the first reported work to obtain the antenna mode characteristic impedance by the antenna theory. While the ETLA approach outperforms the previous frequency-independent solution and requires a reduced complexity over the ATN approach. Our model is general as it converges to the previous model at lower frequencies. Simulation results also show the relationship between the antenna mode characteristic impedance and the power of the interference caused by the current conversion.**

***Index Terms*—Antenna theory, electromagnetic interference, electric field effects, transmission line theory, transmission line modeling, VHF radio communication.**

I. Introduction

Broadband power line communication (BPLC) [1] has drawn much attention of researchers in the last decade as a cost-effective solution for indoor broadband networks. In the IEEE 1901 standard [1], BPLC is allowed to access the frequency band below 100 MHz with restricted power spectral density. Also, it has been proposed in [2] to extend the BPLC bandwidth to cover the whole very high frequency (VHF) band of 30-300 MHz. However, BPLC in the VHF band suffers interference from surrounding wireless services such as TV and radio channels [3] [4]. The current induced by incident electric field has been investigated thoroughly in many electromagnetic compatibility (EMC) applications [5]–[20].

The electromagnetic field can interfere with the VHF BPLC by exciting the antenna mode current [16], also known as the common mode current [14]. In this case, the excited current has the same magnitude and phase which implies that the sum of the transmission line (TL) currents is not equal to zero [16]. The excited antenna mode current can convert to differential one by mode conversion mechanisms [21]. Those mechanisms depend mainly on the imbalance between TLs, which means that the impedance seen by each TL terminal to the ground is not the same [21]. This mode conversion is a significant source of interference to all the differential mode communication signals such as VHF BPLC. In order to evaluate the power converted from the antenna mode to the differential mode at the TL terminals, we have to evaluate the amount of the antenna mode power reflected or transmitted at the terminals, due to the mismatch between the terminal impedance and the antenna mode characteristic impedance. This yields the importance of studying the antenna mode characteristic impedance.

The main approach to describe the antenna mode and the differential mode characteristic impedance is the TL theory, which assumes the existence of three conditions: 1) The cross section of the wire is very small compared to the wavelength of the incident electric field; 2) The propagating field along the wire is either transverse electromagnetic (TEM) or quasi-TEM; c) The sum of the currents propagating along the wire must be equal to zero. If any of those conditions is violated, then the TL theory approach becomes inadequate for modeling the characteristic impedance. In [15]–[20], an approximate TL theory solution was adopted to model the TL characteristic impedance.

When the first condition above is violated, several studies such as [17] and [18] have considered the dependence of the per unit length (p.u.l.) parameters on frequency. However, those studies did not consider the effect of TL length, which makes the solutions presented in [17] and [18] inadequate for the case of thin wire TLs excited by VHF electric field, *e.g.*, the case of electromagnetic interference which is induced across overhead lines or indoor power line cables. Also, the studies presented in [17] and [18] focused only on the differential mode excitation and neglected the antenna mode excitation which is the main source of interference. In [19], an iterative method was proposed to solve the classical TL differential equations based on the perturbation theory. It was proved to have higher accuracy than the classical TL method in [20]. However, the iterative method could diverge at some frequencies. In [16], the authors provided a TL approximated solution for antenna mode characteristic impedance. However,

M. Heggo, X. Zhu and Y. Huang are with the Department of Electrical Engineering and Electronics, University of Liverpool, Liverpool L69 3GJ, UK. E-mails:{m.heggo, xuzhu, huangyi}@liv.ac.uk.

S. Sun is with the Institute for Infocomm Research, Agency for Science, Engineering and Research (A*STAR), Singapore. E-mail: sunsm@i2r.a-star.edu.sg. M. Heggo is also with A*STAR, Singapore.

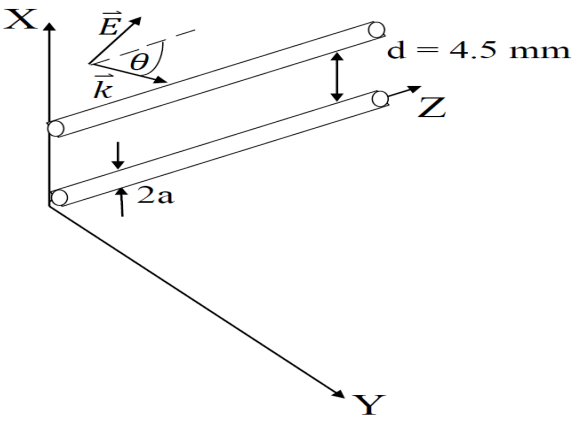

Fig. 1. TL model of straight wires

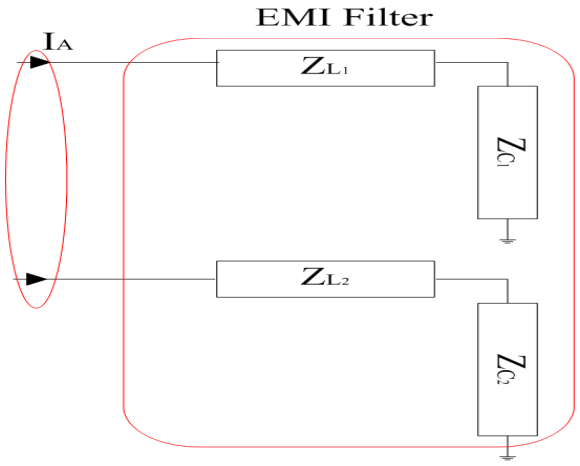

Fig. 2. Two-wire TL terminated with EMI filter

they did not take into consideration the effect of the frequency of operation or the angle of incidence of the electric field. In [22], a full wave transmission line (FWTL) solution was proposed based on Maxwell's theory. The transmission line parameters were expressed using a parameter matrix. Iteration and perturbation methods were used to derive the exact solution for the differential mode current case. The parameter matrix of the transmission line is updated for every iteration, which increases the complexity of the solution when being applied to the antenna mode current case, since the integration formula of the parameter matrix gets more complicated for each iteration.

In our work, a general model is constructed for the VHF current conversion from antenna to differential mode across TLs terminals. The proposed model includes the derivation of a general formula for the characteristic impedance of the antenna mode current. Two approaches are proposed to the formulated problem: 1) Antenna theory numerical (ATN) approach; 2) Enhanced TL approximation (ETLA) analytical approach. The model is important in predicting the amount of antenna mode power transmitted or reflected at the terminals of the TL and hence, the amount of antenna mode interference to the differential mode signals. Our work is different in the following aspects. *First*, we investigate the high frequency (more specifically the VHF) excitation of the antenna mode current. We provide a comprehensive analysis on the antenna mode current characteristic impedance since this is critical for determining the amount of the antenna mode power that converts to the differential mode and causes interference to the differential signal. *Second*, this is the first work to adopt the antenna theory to construct a general ATN solution for representing the antenna mode characteristic impedance. While in [15]–[19], the antenna theory approach was limited to current derivation. *Third*, the ETLA analytical approach is proposed to represent the mean value of the antenna mode current characteristic impedance. Unlike [16], where the characteristic impedance is independent of the exciting frequency effect, our analytical ETLA solution is applicable to the whole VHF band. The proposed solution emphasizes the impact of the exciting frequency and incident angle on the mean value of the antenna mode characteristic impedance.

Section II presents our system model. Section III introduces the antenna theory approach and the construction of the Green's functions for the excited current, volt and magnetic vector potential. Section IV presents the construction of both the ATN and ETLA solutions for representing the antenna mode characteristic impedance. Section V shows the simulation results from our two proposed solutions. Furthermore, the simulation for the mode conversion from antenna to differential mode is presented. Section VI concludes our work.

II. System Model

In this paper, we investigate the case of two parallel straight wires in the free space, as illustrated in Fig. 1. Each wire has a length of 40 m and a radius of 1.5 mm. The distance between the two wires is assumed to be 4.5 mm and the maximum operating frequency is 300 MHz. This means that the transverse dimensions of the wires are electrically small, which satisfies the first two conditions in the TL theory and supports the thin wire approximation. The wires are assumed to be along z-axis. The electric field is assumed to be vertically polarized in the XZ plane where θ represents its angle of incidence on the two wires.

The electromagnetic interference filter (EMI) is a passive device that is used to suppress conducted interference and, is used to protect a device from outside interference or protect the outside environment from unwanted signals generated by the device. However, the asymmetry in the EMI filter with respect to the ground can cause mode conversion between antenna and differential mode signals [21].

In Fig. 2, a two-wire TL terminated by EMI filter is shown. The equivalent circuit is the same as that presented in [23]. $Z_{L1,2}$ represents the equivalent impedance of the EMI filter coil which can be modeled by parallel R-L-C circuit. Also, $Z_{C1,2}$ represents the equivalent impedance of the EMI filter capacitance towards the ground. This capacitance can be modeled by a series R-L-C circuit. All the values of R-L-C are the same as those in [23]. It is assumed that the asymmetry ratio between the transmission line components is 0.3, *i.e.*, the components of the two transmission lines differ from each other by 30% in value. A 100 mA antenna mode current is assumed to be excited by the plane wave along the TL. Since

each TL is terminated with different impedance, each line shows different transmission coefficient. Hence, differential signals will occur across the line terminals leading to the generation of harmful interference. The interference power P_{t_i} can be defined as the power of the differential signal induced by the antenna mode current at the TL terminals, by any of the mode conversion mechanisms. The calculation of P_{t_i} and the model of mode conversion are discussed in detail in Appendix A.

III. Characteristic Green's Functions Construction

In this section, we aim to construct an antenna potential Green's function (APGF) that represents the potential induced along the TL when applying a delta external electric field to a perfect conducting TL in free space. In the same sense, we aim to construct the rest of the characteristic Green's functions like the magnetic vector potential Green's function (MVGF) and the charge density Green's function (CDGF). Using the Green's functions of the antenna potential, the magnetic vector potential, the charge density and the antenna current, we can derive the general solution for the antenna mode characteristic impedance in Section IV.

A. Problem Formulation of Excited Current

The current induced by an electric field incident over a wire is related to the exciting field by the electric field integral equation (EFIE) [24]. Let $\mathbf{E}_t^{ex}$ be the tangential component of the exciting electric field and let $\mathbf{J}$ be the induced current along the length of the wire, then we have

$$\mathbf{E}_t^{ex}(\mathbf{r}) = -j\omega\mu_0 \int_l [\bar{\mathbf{I}} + \frac{1}{k_0^2} \bigtriangledown \bigtriangledown .] \frac{e^{-jk_0|\mathbf{r}-\mathbf{r}'|}}{4\pi|\mathbf{r}-\mathbf{r}'|} . \mathbf{J}(\mathbf{r}') d\mathbf{r}' \quad (1)$$

where $\mathbf{r}'$ and $\mathbf{r}$ are the position vectors of the source and observation points, respectively, l is the length of the wire, $\bar{\mathbf{I}}$ indicates a unit vector, k_0 is the free space wave number where $k_0 = \omega\sqrt{\epsilon_0\mu_0}$. Here, ω is the angular frequency of the exciting electric field, ϵ_0 is the free space electric permittivity and μ_0 is the free space magnetic permeability. The wire is assumed to be a perfect conductor. Hence, the total tangential electric field shall be equal to zero. Also, a thin wire approximation is assumed such that the radius of the wire is too much shorter than the wavelength of the exciting electric field. Here we can consider that the electric field is related to the induced current by the dyadic free space Green's function as

$$\mathbf{E}_t^{ex}(\mathbf{r}) = \int_l G_{EGF}(\mathbf{r}-\mathbf{r}')\mathbf{J}(\mathbf{r}')d\mathbf{r}' \quad (2)$$

where the electric field Green's function $G_{EGF}(\mathbf{r},\mathbf{r}')$ is expressed as

$$G_{EGF}(\mathbf{r},\mathbf{r}') = -j\omega\mu_0[\bar{\mathbf{I}} + \frac{1}{k_0^2} \bigtriangledown \bigtriangledown .] \frac{e^{-jk_0|\mathbf{r}-\mathbf{r}'|}}{4\pi|\mathbf{r}-\mathbf{r}'|} \quad (3)$$

The relation between the exciting electric field and the induced current can be expressed using the operator $\mathcal{L}$ as in [24]

$$\mathbf{E}_t^{ex}(\mathbf{r}) = \mathcal{L}\mathbf{J}(\mathbf{r}') \quad (4)$$

where $\mathcal{L}$ can be expressed as

$$\mathcal{L} = \frac{-j\omega\mu_0}{4\pi} \int_l [\bar{\mathbf{I}} + \frac{1}{k_0^2} \bigtriangledown \bigtriangledown .] G_{\text{fs}}(\mathbf{r},\mathbf{r}')d\mathbf{r}' \quad (5)$$

Hence, the current can be expressed in the terms of the exciting field as

$$\mathbf{J}(\mathbf{r}) = \mathcal{L}^{-1}\mathbf{E}_t^{ex}(\mathbf{r}') \quad (6)$$

This means that the excited current can be obtained using the integration of a Green's function with the exciting electric field. The antenna current Green's function was derived in [24] using the distribution theory. It was expressed as the distribution of a series of dyadic antenna current Green's functions $\bar{\mathbf{F}}_n(\mathbf{r},\mathbf{r}')$ over the electric field as a test function. $\bar{\mathbf{F}}_n(\mathbf{r},\mathbf{r}')$ can be derived using the operator $\mathcal{L}_{\mathbf{r}}^{-1}$, where the subscript $\mathbf{r}$ in the operator $\mathcal{L}_{\mathbf{r}}^{-1}$ indicates that the operator $\mathcal{L}^{-1}$ is applied to vector $\mathbf{r}$. Hence, $\bar{\mathbf{F}}_n(\mathbf{r},\mathbf{r}')$ can be expressed as

$$\bar{\mathbf{F}}_n(\mathbf{r},\mathbf{r}') = \mathcal{L}_{\mathbf{r}}^{-1} f_n^S(\mathbf{r},\mathbf{r}') \quad (7)$$

where $f_n^S(\mathbf{r},\mathbf{r}')$ is a series of non-negative locally integrable functions along the wire. S is the two-dimensional manifold space, where $f_n^S(\mathbf{r},\mathbf{r}')$ functions are defined. Those functions shall satisfy the conditions as defined in Theorem A.1 of Appendix A in [24]. Also, if the operator $\mathcal{L}^{-1}$ is applied to vector $\mathbf{r}'$ or $\mathbf{r}''$ function the operator shall be $\mathcal{L}_{\mathbf{r}'}^{-1}$ or $\mathcal{L}_{\mathbf{r}''}^{-1}$, respectively. For thin wire approximation, the series of functions $f_n^S(\mathbf{r},\mathbf{r}')$ converges to $\delta(\mathbf{r}-\mathbf{r}')$ as $n \to \infty$. Hence, it can be shown

$$\mathcal{L}_{\mathbf{r}}^{-1}\delta(\mathbf{r}-\mathbf{r}') = \lim_{n\to\infty} \mathcal{L}_{\mathbf{r}}^{-1} f_n^S(\mathbf{r},\mathbf{r}') \quad (8)$$

Hence, the current can be expressed as

$$\mathbf{J}(\mathbf{r}) = \lim_{n\to\infty} \langle \bar{\mathbf{F}}_n(\mathbf{r},\mathbf{r}')\mathbf{E}_t^{ex}(\mathbf{r}') \rangle \quad (9)$$

This can be interpreted for the case of a thin wire in the integral form as

$$\mathbf{J}(\mathbf{r}) = \lim_{n\to\infty} \int_l \bar{\mathbf{F}}_n(\mathbf{r},\mathbf{r}')\mathbf{E}_t^{ex}(\mathbf{r}')d\mathbf{r}' \quad (10)$$

This means that according to the distribution theory, the distribution of $\bar{\mathbf{F}}_n(\mathbf{r},\mathbf{r}')$ over electric field can converge to

$$\mathbf{J}(\mathbf{r}) = \int_l \mathcal{L}_{\mathbf{r}}^{-1}\delta(\mathbf{r}-\mathbf{r}')\mathbf{E}_t^{ex}(\mathbf{r}')d\mathbf{r}' \quad (11)$$

Hence, the final expression for the antenna current Green's function G_{AC} is

$$G_{\text{AC}}(\mathbf{r},\mathbf{r}') = \mathcal{L}_{\mathbf{r}}^{-1}\delta(\mathbf{r}-\mathbf{r}') \quad (12)$$

B. Construction of Green's Function of the Charge Density, the Antenna Potential and the Magnetic Vector Potential

1) Charge Density Green's function: The charge density $\rho(\mathbf{r})$ can be expressed using the continuity equation as

$$\rho(\mathbf{r}) = \frac{-1}{j\omega} \frac{\partial \mathbf{J}(\mathbf{r})}{\partial \mathbf{r}} \quad (13)$$

Applying (11) in (13), we get

$$\rho(\mathbf{r}) = \frac{-1}{j\omega} \frac{\partial}{\partial \mathbf{r}} \int_l \mathcal{L}_{\mathbf{r}}^{-1}\delta(\mathbf{r}-\mathbf{r}')\mathbf{E}_t^{ex}(\mathbf{r}')d\mathbf{r}' \quad (14)$$

We can conclude the charge density Green's function G_{CD} as

$$G_{\text{CD}}(\mathbf{r},\mathbf{r}') = \frac{-1}{j\omega}\frac{\partial}{\partial \mathbf{r}} G_{\text{AC}}(\mathbf{r},\mathbf{r}') \tag{15}$$

2) Antenna Potential Green's function: Let $\phi(\mathbf{r})$ be the retarded scalar potential. Also, let $\mathbf{r}''$ be the position vector of the impressed excitation electric field, $\mathbf{r}'$ be the position vector for the excited current and $\mathbf{r}$ be the position vector for the observation point of induced potential. We can find an expression for the antenna potential Green's function as

$$\phi(\mathbf{r}) = \frac{1}{4\pi\epsilon_0}\int_l G_{\text{fs}}(\mathbf{r},\mathbf{r}')\rho(\mathbf{r}')d\mathbf{r}' \tag{16}$$

where $G_{\text{fs}}(\mathbf{r},\mathbf{r}')$ is free space Green's function described by

$$G_{\text{fs}}(\mathbf{r},\mathbf{r}') = \frac{e^{-jk_0|\mathbf{r}-\mathbf{r}'|}}{|\mathbf{r}-\mathbf{r}'|} \tag{17}$$

Substituting (11) and (13) into (16), we get

$$\phi(\mathbf{r}) = \frac{-1}{4\pi\epsilon_0 j\omega}\int_l\int_l G_{\text{fs}}(\mathbf{r},\mathbf{r}')\frac{\partial}{\partial \mathbf{r}'}\mathcal{L}^{-1}_{r'}\delta(\mathbf{r}'-\mathbf{r}'')\mathbf{E}^{ex}_t(\mathbf{r}'')d\mathbf{r}''d\mathbf{r}' \tag{18}$$

Using (12) and (18), we can conclude the final expression for the antenna potential Green's function G_{AV} as

$$G_{\text{AV}}(\mathbf{r},\mathbf{r}'') = \frac{-1}{4\pi\epsilon_0 j\omega}\int_l G_{\text{fs}}(\mathbf{r},\mathbf{r}')\frac{\partial}{\partial \mathbf{r}'}G_{\text{AC}}(\mathbf{r}',\mathbf{r}'')d\mathbf{r}' \tag{19}$$

3) Magnetic Vector Potential Green's function: Using an approach similar to the above, we find the magnetic vector potential Green's function. Let $\mathbf{A}(\mathbf{r})$ be the magnetic vector potential which can be expressed as

$$\mathbf{A}(\mathbf{r}) = \frac{\mu_0}{4\pi}\int_l G_{\text{fs}}(\mathbf{r},\mathbf{r}')\mathbf{J}(\mathbf{r}')d\mathbf{r}' \tag{20}$$

Substituting (11) into (20) yields

$$\mathbf{A}(\mathbf{r}) = \frac{\mu_0}{4\pi}\int_l\int_l G_{\text{fs}}(\mathbf{r},\mathbf{r}')\mathcal{L}^{-1}_{r'}\delta(\mathbf{r}'-\mathbf{r}'')\mathbf{E}^{ex}_t(\mathbf{r}'')d\mathbf{r}''d\mathbf{r}' \tag{21}$$

Also substituting (12) into (21), the final expression for the magnetic vector potential Green's function G_{MV} can be stated as

$$G_{\text{MV}}(\mathbf{r},\mathbf{r}'') = \frac{\mu_0}{4\pi}\int_l G_{\text{fs}}(\mathbf{r},\mathbf{r}')G_{\text{AC}}(\mathbf{r}',\mathbf{r}'')d\mathbf{r}' \tag{22}$$

IV. The ATN and ETLA Approaches for Characteristic Impedance Construction of The Antenna Mode Current

In this section, we propose the ATN and ETLA approaches for representing the characteristic impedance of the antenna mode current. We derive the direct relations between the characteristic impedance and the exciting field incident over two perfect conducting wires in free space.

A. The ATN Approach for Characteristic Impedance

In this part, we propose the general ATN solution for the characteristic impedance. We use the Green's functions of the antenna potential, the magnetic vector potential and antenna current derived in Section III throughout our derivation. The capacitance p.u.l. $C_{\text{d/a}}$ can be defined as [25]

$$C_{\text{d/a}}(\mathbf{r}) = \frac{\rho_{\text{d/a}}(\mathbf{r})}{\phi_{\text{d/a}}(\mathbf{r})} \tag{23}$$

where the subscript d/a indicates the differential or antenna mode of excitation. Using (14), (15), (18) and (19), (23) can be written as

$$C_{\text{d/a}}(\mathbf{r}) = \frac{\int_l G_{\text{CD}-\text{d/a}}(\mathbf{r},\mathbf{r}')\mathbf{E}^{ex}_t(\mathbf{r}')d\mathbf{r}'}{\int_l G_{\text{AV}-\text{d/a}}(\mathbf{r},\mathbf{r}'')\mathbf{E}^{ex}_t(\mathbf{r}'')d\mathbf{r}''} \tag{24}$$

Also, the inductance p.u.l. $L_{\text{d/a}}$ can be defined as [25]

$$L_{\text{d/a}}(\mathbf{r}) = \frac{\mathbf{A}_{\text{d/a}}(\mathbf{r})}{\mathbf{J}_{\text{d/a}}(\mathbf{r})} \tag{25}$$

Using (21), (22), (11) and (12), (25) can be written as

$$L_{\text{d/a}}(\mathbf{r}) = \frac{\int_l G_{\text{MV}-\text{d/a}}(\mathbf{r},\mathbf{r}'')\mathbf{E}^{ex}_t(\mathbf{r}'')d\mathbf{r}''}{\int_l G_{\text{AC}-\text{d/a}}(\mathbf{r},\mathbf{r}')\mathbf{E}^{ex}_t(\mathbf{r}')d\mathbf{r}'} \tag{26}$$

where $G_{\text{CD}-\text{d/a}}$, $G_{\text{AV}-\text{d/a}}$, $G_{\text{MV}-\text{d/a}}$ and $G_{\text{AC}-\text{d/a}}$ are precisely defined in Appendix B.

It is worth mentioning that our numerical ATN solution uses the approximated method of moments (MOM) numerical form of equations (24) and (26), where the boundary condition matrix is represented. The boundary condition matrix is forcing the boundary conditions at the TL terminals. Using matrix operations, the boundary condition matrix is eliminated from the numerator and denominator so that the p.u.l. parameters are independent of the boundary conditions at the TL terminals. The complete proof of the boundary condition matrix elimination is shown in Appendix C.

Equations (24) and (26) provide a general integral form for the capacitance and inductance p.u.l., respectively. Since we are concerned about the behavior of the antenna mode characteristic impedance for lossless conductors in free space, we can define the characteristic impedance $Z(\mathbf{r})$ as

$$Z(\mathbf{r}) = \sqrt{\frac{L_{\text{d/a}}(\mathbf{r})}{C_{\text{d/a}}(\mathbf{r})}} \tag{27}$$

B. The ETLA Approach for the Mean Value of the Antenna Mode Characteristic Impedance

Due to the complexity of the ATN approach using the antenna theory, we present an ETLA approach based on a modified TL approach. Although the first two conditions of the TL theory are still satisfied in the antenna mode current case under consideration, the third condition is not satisfied (*i.e.*, the sum of the currents is not equal to zero). Hence, the ETLA approach adopts an approximation for the TL theory to represent the mean value of the antenna mode characteristic

impedance, taking into consideration the frequency of operation and angle of incidence. We can define $\Psi(\mathbf{r})$ as

$$\begin{aligned}\Psi(\mathbf{r}) = \\ &- 0.9.\{j\pi H_0^{(2)}(a\sqrt{k_0^2-k_1^2}) + j\pi H_0^{(2)}(d\sqrt{k_0^2-k_1^2})\} \\ &- 2\{E_1(j(l-r+a)(k_0-k_1)) + E_1(j(r+a)(k_0+k_1))\}\end{aligned} \tag{28}$$

where $H_0^{(2)}(x)$ denotes the Hankel function of the zero-th order and second kind, $E_1(z)$ is the exponential integral function, d is the distance between the two wires of the TL. a is the radius of each wire in the TL and $k_1 = k_0\cos(\theta)$, where θ is the incidence angle. Hence, the inductance and the capacitance p.u.l. can be expressed as

$$L_a(\mathbf{r}) = \frac{\mu_0\Psi(\mathbf{r})}{4\pi} \tag{29}$$

$$C_a(\mathbf{r}) = \frac{4\pi\epsilon_0}{\Psi(\mathbf{r})} \tag{30}$$

where the subscript a refers to the antenna mode of excitation. Subistituting (29) and (30) into (27) yields

$$Z(\mathbf{r}) = \frac{\Psi(\mathbf{r})}{4\pi}\sqrt{\frac{\mu_0}{\epsilon_0}} \tag{31}$$

The full derivation of the ETLA solution can be found in Appendix D. It can be easily concluded that the characteristic impedance depends mainly on the value of $\Psi(\mathbf{r})$. Here we shall refer to two important parameters that affect $Z(\mathbf{r})$: 1) Frequency; 2) Incidence angle and discuss their relationships in the following:

1) $Z(\mathbf{r})$ vs. Frequency: As mentioned before, $\Psi(\mathbf{r})$ has been derived on the basis that the wire length is much more than the operating wavelength. Hence, we can intuitively conclude from (28), that $\Psi(\mathbf{r})$ decreases as the frequency increases. This is due to the fact that when the frequency increases, the wavelength decreases and both k_0 and k_1 increase, and hence, both the Hankel functions and the exponential integral functions decrease.

2) $Z(\mathbf{r})$ vs. Incidence Angle: Incidence angle has inverse relationship with the value of k_1. Consequently, as the incidence angle increases, $k_0 - k_1$ increases while $k_0 + k_1$ decreases. This leads to the decrease of $H_0^{(2)}(a\sqrt{k_0^2-k_1^2})$, $H_0^{(2)}(d\sqrt{k_0^2-k_1^2})$ and $E_1(j(l-r+a)(k_0-k_1))$ and the increase of $E_1(j(r+a)(k_0+k_1))$. Hence, the variation of the incident angle does not yield a significant variation of the characteristic impedance mean value.

V. Simulation Results

In (27) and (31), we have proposed the ATN and ETLA solutions for the antenna mode characteristic impedance. In this section, we present their performance by simulation, in comparison to the classical TL solution in [16]. We use the formulae presented in [16] for the inductance and the capacitance p.u.l. of the antenna mode current to derive the TL antenna mode characteristic impedance. Also, we present a performance comparison between our proposed solutions and the FWTL solution, which was proposed in [22] to derive the differential mode current and its characteristic parameter matrix. However, in our simulations we use the FWTL solution in order to derive the antenna mode characteristic impedance, where the relation between the characteristic impedance and the characteristic parameter matrix is defined according to [26].

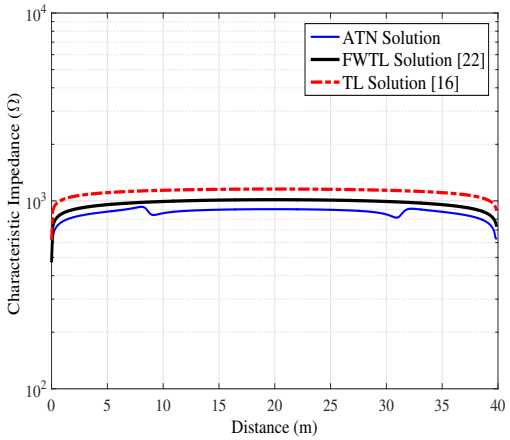

Fig. 3. Characteristic impedance at frequency 2 MHz and $\theta = 30°$.

A. Characteristic Impedance vs. Frequency

In Fig. 3, the characteristic impedance is shown using our ATN solution for the antenna mode of excitation at frequency of 2 MHz and angle of incidence $\theta = 30°$. The wavelength of operation is 150 m which is much more than the wire length. It can be observed that both our ATN solution and the FWTL solution converge to the TL solution in [16] at low frequency of 2 MHz, proving the validity of our solution. Also, it can be easily observed that the difference between the ATN and the TL solutions approaches 157 Ω. This is due to the difference between our ATN procedure and the TL approximation adopted in [16], where the ATN numerical approach gives the exact solution for the characteristic impedance and the TL approach gives an approximated value. We shall take into consideration that the antenna mode Green's function in equation (36) is not fast decaying as the differential mode one, which increases the approximation error in the TL approach. This makes the difference between our solution and that in [16] easily justified.

In Fig. 4, the characteristic impedance is shown versus the distance along the wire. We compare the performance of our ATN solution at different frequencies of 30, 100 and 300 MHz (the corresponding wavelengths are all shorter than the wire length) to the performance of the TL solution in [16]. It can be observed the effect of the frequency on changing the mean value of the characteristic impedance.

In Fig. 5, the characteristic impedance versus frequency is shown at a fixed position of 30 meters from the origin and at an angle of incidence of $\theta = 45°$. The characteristic impedance obtained from ATN, FWTL and ETLA solutions decreases with the increase in the frequency, while the TL solution [16] presents a frequency-independent characteristic

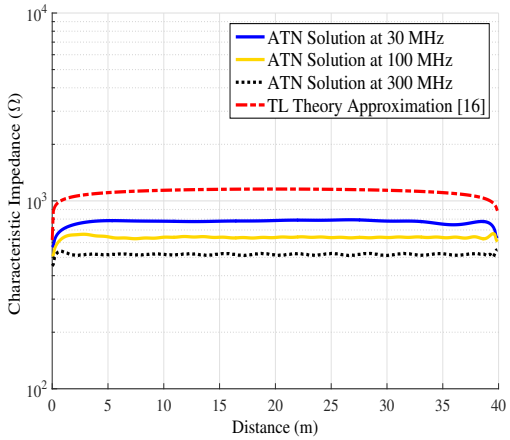

Fig. 4. Characteristic impedance vs. distance along the wire length at incident angle $\theta = 45°$.

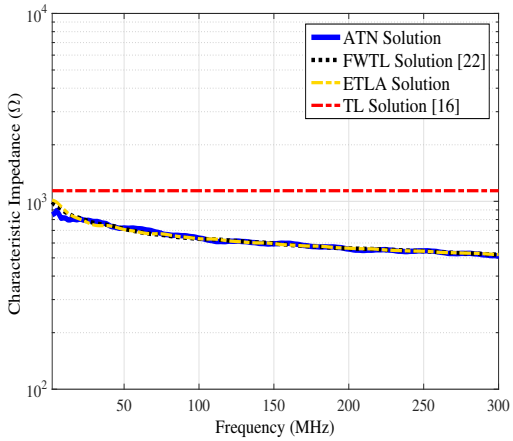

Fig. 5. Characteristic impedance vs. frequency at a distance 30 m from the origin and $\theta = 45°$.

impedance. This verifies our analysis in Subsection IV-B.

In Fig. 6, the characteristic impedance of the antenna mode current is shown versus the frequency of different geometric structures for the two straight wires in free space. In the simulations, three geometric structures with different values

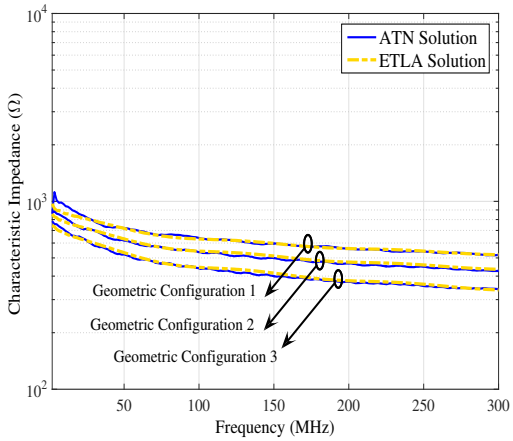

Fig. 6. Characteristic impedance vs. frequency for different geometric structures.

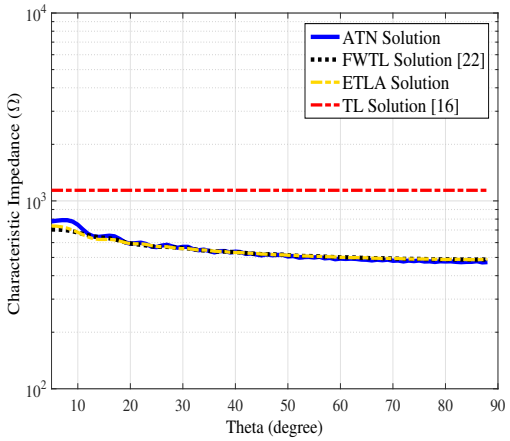

Fig. 7. Characteristic impedance vs. angle of incidence θ at a distance 30 m from the origin and frequency 100 MHz.

of wire length (l), radius (a) and separation distance (d) have been considered. The three geometric structures 1, 2 and 3 have the geometric parameter combination (l, a, d) as: (40, 1.5×10^{-3}, 4.5×10^{-3}) m, (60, 2×10^{-3}, 1.8×10^{-3}) m and (80, 3×10^{-2}, 8.1×10^{-2}) m. It can be observed that for different geometric structures, the antenna mode characteristic impedance still decreases with the frequency increase. This proves that in the VHF band (more specifically when the $\lambda < l$, where λ is the exciting wavelength) the antenna mode characteristic impedance decreases with the increase in the frequency regardless of the geometric structure.

B. Characteristic Impedance vs. Incidence Angle

The effect of the incident angle on the mean value of the characteristic impedance is smaller than that of the frequency. This is demonstrated in Fig. 7. The simulation results show that the angle of incidence has a smaller effect on the mean value of the characteristic impedance compared to the effect of the exciting frequency. This agrees with our analysis in Section IV-B. In Fig. 7, the difference between the simulation results obtained using our proposed solutions and the TL solution [16] is due to the fact that the simulation is done at 100 MHz. As mentioned before, the TL solution is not applicable to high frequency.

In Fig. 8, the characteristic impedance of the antenna mode current is shown versus the incident angle for different geometric structures. The simulation results show that the geometric structure does not affect the performance of the antenna mode characteristic impedance towards the change in the incident angle.

C. Antenna Mode Interference to Differential Mode Signal

The antenna mode current can convert to differential mode by mode conversion mechanisms [21] [27] [28]. The adopted mode conversion mechanism is discussed in Appendix A. In Figs. 9 and 10, the calculation of the converted interference signal from antenna mode to differential mode is presented at different frequencies. In Fig. 9, the interference power is calculated for different EMI filter locations across the TL,

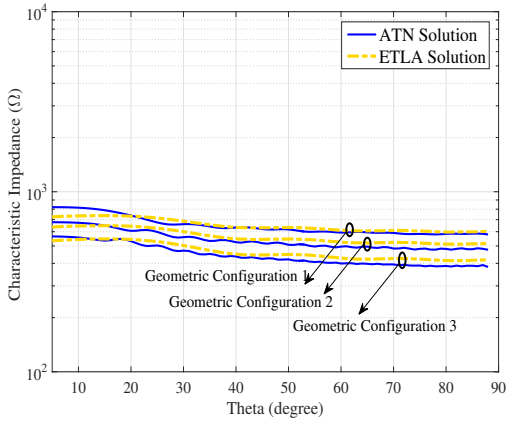

Fig. 8. Characteristic impedance vs. angle of incidence θ for different geometric structures.

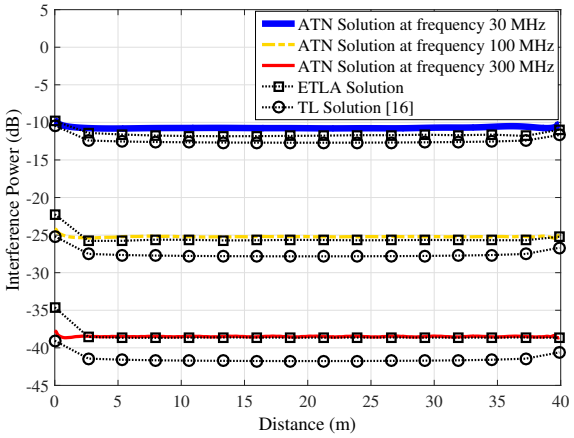

Fig. 9. Interference power vs. distance at different frequencies for incidence angle $\theta = 45°$.

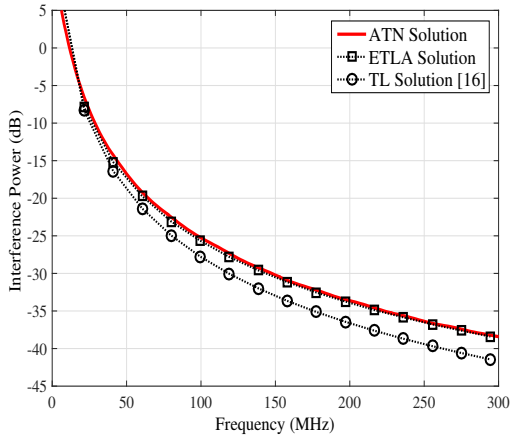

Fig. 10. Interference power vs. frequency at incident angle $\theta = 45°$.

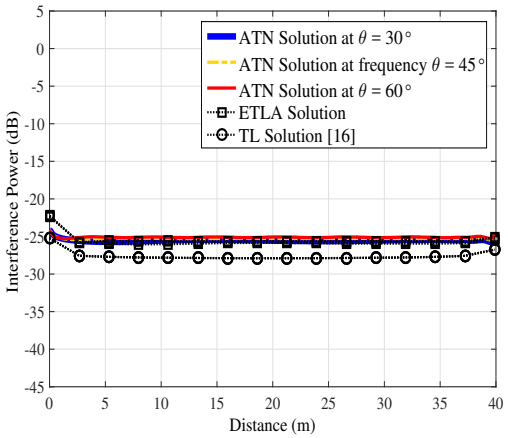

Fig. 11. Interference power vs. distance at different incident angles for frequency of 100 MHz.

where the distance is measured from the origin to the location of the EMI filter. The interference power reduces with the increase of frequency, but is relatively stable at different distances. It can be observed that our proposed solutions yield a higher calculated interference power at different frequencies than that in [16]. The difference between the ETLA approach and the TL approach in [16] reaches more than 4 dB at 300 MHz, which means more than double the interference power. This is because our proposed solution has lower antenna mode characteristic impedance than that proposed in [16].

In Fig. 11, the interference power at different incident angles for the same frequency of operation is shown. It can be observed that the interference mean value is not much affected by the incident angle.

VI. Conclusion

The antenna mode interference to the differential mode signal has a great influence on a number of EMC applications such as BPLC in the VHF band. In this paper, two solutions (ATN and ETLA) for representing the characteristic impedance of the excited antenna mode current in the VHF band have been proposed. The ATN solution has been shown to be dependent on the exciting frequency and incidence angle, unlike the TL solution in [16] which is independent of the two parameters. Also, the ATN solution matches the FWTL solution in [22], while directly deriving the impedance without the need to derive the current as the FWTL solution. Furthermore, the ETLA solution shows a negligible difference from the ATN and FWTL solutions, while requiring a lower computational complexity. Our proposed solutions show a higher interference power across a TL terminated by EMI filter than the TL solution in [16]. This will help in providing a more accurate estimation of the power of the antenna mode interference to the differential mode signal.

Appendix A
Modelling the Antenna Mode Current Conversion to Differential Mode

The antenna mode current is converted to differential mode due to the asymmetry of the terminal loads as in [21] [27] [28].

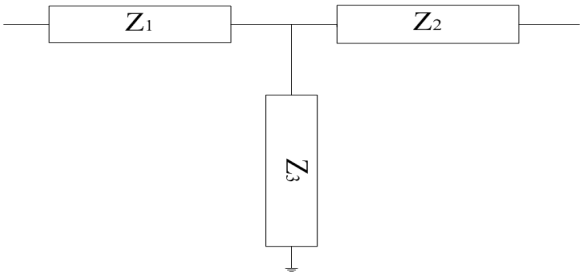

Fig. 12. T-network terminal impedance

As shown in Fig. 12, a T-network is adopted to represent the impedance asymmetry at the TL terminals. Let ϕ_{a_t} and ϕ_{d_t} be the generated antenna and differential mode potentials at the terminal loads. Also, let J_{a_t} and J_{d_t} be the values of the antenna and differential mode currents transmitted to the terminal loads. The conversion between the different modes of current propagating along the TL can be written as

$$\begin{bmatrix}\phi_{a_t}\\ \phi_{d_t}\end{bmatrix} = \begin{bmatrix}Z_{a_t} & \triangle Z_t\\ \triangle Z_t & Z_{d_t}\end{bmatrix}\begin{bmatrix}J_{a_t}\\ J_{d_t}\end{bmatrix} \tag{32}$$

where Z_{a_t} and Z_{d_t} are the equivalent antenna mode and differential mode impedance at the terminal loads, respectively. The relationship between Z_{a_t}, Z_{d_t} and Z_1, Z_2, Z_3 is defined as in [27] [28]. $\triangle Z_t$ is the difference between the values of the impedance seen by each transmission line to the ground. The relationship between the terminal load currents J_{a_t}, J_{d_t} and the TL currents J_a, J_d can be expressed as

$$\begin{bmatrix}J_{a_t}\\ J_{d_t}\end{bmatrix} = \begin{bmatrix}T_{a_t} & 0\\ 0 & T_{d_t}\end{bmatrix}\begin{bmatrix}J_a\\ J_d\end{bmatrix} \tag{33}$$

where T_{a_t} and T_{d_t} are the transmission coefficients of the both the antenna mode and differential mode current at the terminal loads.

Hence, the differential interference potential $\phi_{d_{t_i}}$ induced due to the antenna mode current is expressed as

$$\phi_{d_{t_i}} = \triangle Z_t T_{a_t} J_a \tag{34}$$

The interference power P_{t_i} can be calculated as

$$P_{t_i} = \phi_{d_{t_i}} J_{a_t} \tag{35}$$

Appendix B
Green's Function of Antenna Potential, Magnetic Vector Potential and Antenna current for Differential and Antenna Modes of Excitation

Consider the case of two perfect conducting parallel wires. Let $\mathbf{r_1}$ and $\mathbf{r_2}$ be the position vectors for the observation points located on wires, 1 and 2, respectively. Let $\mathbf{r'_1}$ and $\mathbf{r'_2}$ are the position vectors for the source points located on wire 1 and 2, respectively. Free space Green's function $G_{\text{fs}}(\mathbf{r},\mathbf{r}')$ for the differential/antenna (d/a) mode can be defined as

$$G_{\text{fs}-\text{d/a}}(\mathbf{r},\mathbf{r}') = \frac{e^{-jk_0|\mathbf{r}-\mathbf{r'_1}|}}{|\mathbf{r}-\mathbf{r'_1}|}(\overset{-}{+})\frac{e^{-jk_0|\mathbf{r}-\mathbf{r'_2}|}}{|\mathbf{r}-\mathbf{r'_2}|} \tag{36}$$

Hence the $\mathcal{L}$ operator for the differential mode can be defined as

$$\mathcal{L}_{\text{d/a}} = \frac{-j\omega\mu_0}{4\pi}\int_l [\bar{\mathbf{I}} + \frac{1}{k_0^2}\bigtriangledown\bigtriangledown.]G_{\text{fs}-\text{d/a}}(\mathbf{r},\mathbf{r}')d\mathbf{r}' \tag{37}$$

Hence we can define the Green's functions of the antenna current , the antenna potential, the magnetic vector potential and the charge density for the differential or antenna mode of excitation as

$$G_{\text{AC}-\text{d/a}}(\mathbf{r},\mathbf{r}') = \mathcal{L}_{\text{d/a}r}^{-1}\delta(\mathbf{r}-\mathbf{r}') \tag{38}$$

$$G_{\text{AV}-\text{d/a}}(\mathbf{r},\mathbf{r}'') = \frac{-1}{4\pi\epsilon_0 j\omega}\int_l G_{\text{fs}-\text{d/a}}(\mathbf{r},\mathbf{r}')\frac{\partial}{\partial\mathbf{r}'}\mathcal{L}_{r'-\text{d/a}}^{-1}\delta(\mathbf{r}'-\mathbf{r}'')d\mathbf{r}' \tag{39}$$

$$G_{\text{MV}-\text{d/a}}(\mathbf{r},\mathbf{r}'') = \frac{\mu_0}{4\pi}\int_l G_{\text{fs}-\text{d/a}}(\mathbf{r},\mathbf{r}')\mathcal{L}_{r'-\text{d/a}}^{-1}\delta(\mathbf{r}'-\mathbf{r}'')d\mathbf{r}' \tag{40}$$

$$G_{\text{CD}-\text{d/a}}(\mathbf{r},\mathbf{r}') = \frac{-1}{j\omega}\frac{\partial}{\partial\mathbf{r}}\mathcal{L}_{r-\text{d/a}}^{-1}\delta(\mathbf{r}-\mathbf{r}') \tag{41}$$

Appendix C
Boundary Condition Matrix Elemination

Let $\mathbf{Q}$ be a diagonal matrix which forces the boundary conditions on the excited current at the terminals of the transmission line as presented in [29]. Using the MOM numerical method to solve the integral in equation (20) as in [29], equation (20) is rewritten in the numerical form as

$$\mathbf{A}(\mathbf{r}) = \frac{\mu_0}{4\pi}\mathbf{UQJ}(\mathbf{r}) \tag{42}$$

where $\mathbf{U}$ represents the matrix of integrations of the free space Green's function $G_{\text{fs}}(\mathbf{r},\mathbf{r}')$ with current basis function for different source and observation points. $\mathbf{J}(\mathbf{r})$ is a vector which represents the excited current value at different source points. $\mathbf{J}(\mathbf{r})$ represents the current component which is independent of the boundary conditions, while the effect of the forward and reflected current components are represented in the $\mathbf{Q}$ diagonal matrix. It is worth mentioning that both $\mathbf{U}$ and $\mathbf{Q}$ are symmetric matrices such that $\mathbf{U^T} = \mathbf{U}$ and $\mathbf{Q^T} = \mathbf{Q}$. Equation (25) can be rewritten in the numerical form as

$$L_{\text{d/a}}(\mathbf{r}) = \frac{\frac{\mu_0}{4\pi}\mathbf{UQJ}(\mathbf{r})}{\mathbf{QJ}(\mathbf{r})} \tag{43}$$

Using the symmetry property of $\mathbf{U}$ and $\mathbf{Q}$, equation (43) can be rewritten as

$$L_{\text{d/a}}(\mathbf{r}) = \frac{\frac{\mu_0}{4\pi}\mathbf{QUJ}(\mathbf{r})}{\mathbf{QJ}(\mathbf{r})} \tag{44}$$

The boundary condition matrix can be removed from both numerator and denominator, since $\mathbf{Q}$ matrix is a diagonal matrix. Hence, the above equation is written as

$$L_{\text{d/a}}(\mathbf{r}) = \frac{\frac{\mu_0}{4\pi}\mathbf{UJ}(\mathbf{r})}{\mathbf{J}(\mathbf{r})} \tag{45}$$

Following the same principle the boundary condition matrix can be removed from the numerical form of equation (23) for the capacity p.u.l..

APPENDIX D
DERIVATION OF THE ETLA SOLUTION OF THE ANTENNA MODE CHARACTERISTIC IMPEDANCE MEAN VALUE

The exciting electric field $\mathbf{E}_t^{ex}(\mathbf{r})$ can be expressed in the terms of the potential $\phi(\mathbf{r})$ and the magnetic vector potential $\mathbf{A}(\mathbf{r})$ as

$$\mathbf{E}_t^{ex}(\mathbf{r}) = -j\omega\mathbf{A}(\mathbf{r}) - \nabla\phi(\mathbf{r}) \tag{46}$$

Using both (16) and (46) the general Telegrapher equations for the current induced along two parallel wires in free space by the effect of incident electric field are expressed as

$$\frac{\partial\phi_a(\mathbf{r})}{\partial\mathbf{r}} + \frac{j\omega\mu_0}{4\pi}\int_l G_{\text{fs}-a}(\mathbf{r},\mathbf{r}')\mathbf{J}_a(\mathbf{r}')d\mathbf{r}' = \mathbf{E}_{t-a}^{ex}(\mathbf{r}) \tag{47}$$

$$\phi_a(\mathbf{r}) = -\frac{1}{j\omega 4\pi\epsilon_0}\frac{\partial}{\partial\mathbf{r}}\int_l G_{\text{fs}-a}(\mathbf{r},\mathbf{r}')\mathbf{J}_a(\mathbf{r}')d\mathbf{r}' \tag{48}$$

where $\phi_a(\mathbf{r})$ and $\mathbf{J}_a(\mathbf{r})$ are the excited antenna mode potential and current, respectively.

In case $l < \lambda$ (where λ represents the wavelength), we can consider the current as constant along the integral and apply the approximation used in [16]. However, if $l > \lambda$, the approximation made in [16] becomes invalid and we shall look for a better approximation. Here we assume that the current has two separate components $\mathbf{J}_o(\mathbf{r})$ and $e^{-jk_1\mathbf{r}}$

$$\mathbf{J}_a(\mathbf{r}) = \mathbf{J}_o(\mathbf{r})e^{-jk_1\mathbf{r}} \tag{49}$$

where the rate of change of $\mathbf{J}_o(\mathbf{r})$ with the position vector $\mathbf{r}$ is much less than the decay rate of the free space Green's function $G_{\text{fs}-a}(\mathbf{r},\mathbf{r}')$, so it can be considered as constant over the integral. Also $k_1 = k_o cos(\theta)$ where k_o is the wave number in free space and θ is the incident angle. The integral in equations (47) and (48) can be rewritten as

$$\begin{aligned}&\int_l G_{\text{fs}-a}(\mathbf{r},\mathbf{r}')\mathbf{J}_a(\mathbf{r}')d\mathbf{r}' = \\ &\mathbf{J}_o(\mathbf{r})\int_l \frac{e^{-jk_0|\mathbf{r}-\mathbf{r}_1'|}}{|\mathbf{r}-\mathbf{r}_1'|} + \frac{e^{-jk_0|\mathbf{r}-\mathbf{r}_2'|}}{|\mathbf{r}-\mathbf{r}_2'|}e^{-jk_1\mathbf{r}'}d\mathbf{r}'\end{aligned} \tag{50}$$

Assume that the two wires are along the z-axis. Thus (50) reduces to

$$\begin{aligned}&\int_l G_{\text{fs}-a}(\mathbf{z},\mathbf{z}')\mathbf{J}(\mathbf{z}')d\mathbf{z}' = \\ &\mathbf{J}_o(\mathbf{z})\int_l \left[\frac{e^{-jk_0\sqrt{(\mathbf{z}-\mathbf{z}')^2+a^2}}}{\sqrt{(\mathbf{z}-\mathbf{z}')^2+a^2}} + \frac{e^{-jk_0\sqrt{(\mathbf{z}-\mathbf{z}')^2+d^2}}}{\sqrt{(\mathbf{z}-\mathbf{z}')^2+d^2}}\right]e^{-jk_1\mathbf{z}'}d\mathbf{z}'\end{aligned} \tag{51}$$

where a is the wire radius and d is the distance between the two wires. Substitute $\mathbf{u} = \mathbf{z}' - \mathbf{z}$ into (51) we get

$$\begin{aligned}&\int_l G_{\text{fs}-a}(\mathbf{z},\mathbf{z}')\mathbf{J}(\mathbf{z}')d\mathbf{z}' = \\ &\mathbf{J}_o(\mathbf{z})e^{-jk_1\mathbf{z}}\int_{-z}^{l-z}\left[\frac{e^{-jk_0\sqrt{\mathbf{u}^2+a^2}}}{\sqrt{\mathbf{u}^2+a^2}} + \frac{e^{-jk_0\sqrt{\mathbf{u}^2+d^2}}}{\sqrt{\mathbf{u}^2+d^2}}\right]e^{-jk_1\mathbf{u}}d\mathbf{u}\end{aligned} \tag{52}$$

we can use the following two known integrals

$$\int_{-\infty}^{\infty}\frac{e^{-jk_0\sqrt{u^2+a^2}}}{\sqrt{u^2+a^2}}e^{-jk_1u} = -j\pi H_0^{(2)}(a\sqrt{k_0^2-k_1^2}) \tag{53}$$

and

$$E_1(z) = \int_z^{\infty}\frac{e^{-t}}{t}dt \tag{54}$$

Using (53) and (54) to solve the integral in (52), we can conclude

$$\int_l G_{\text{fs}-a}(\mathbf{r},\mathbf{r}')\mathbf{J}(\mathbf{r}')d\mathbf{r}' = \mathbf{J}(\mathbf{r})\Psi(\mathbf{r}) \tag{55}$$

where $\Psi(\mathbf{r})$ is given by (28).

We added a 0.9 fitting factor to the approximated analytical solution in (28) since we observed a difference between our approximated solution and the numerical solution of the integral in (52). This difference comes from the adopted approximation that the area covered by the integral in (52) is equal to the difference between the areas covered by integrals in (53) and (54). Substituting (28) into (47) and (48), we can obtain the inductance and capacitance p.u.l. in (29) and (30), respectively, and the characteristic impedance in (31).

Discussion on the ETLA approximation: The assumption of the antenna mode current in (49) does not consider two other components of the current which represent the travelling and reflected currents at the TL terminals as discussed in [19]. This is due to the small effect of those current components on the value of the antenna mode characteristic impedance in the VHF band. This small effect can be concluded from the small difference of the ETLA solution compared to both the ATN and FWTL solutions in the simulation results shown in Figs. 3-8.

REFERENCES

[1] L. T. Berger, A. Schwager, P. Pagani, and D. Schneider, *MIMO Power Line Communications: Narrow and Broadband Standards, EMC, and Advanced Processing*. CRC Press, 2014.

[2] M. U. Rehman, S. Wang, Y. Liu, S. Chen, X. Chen, and C. G. Parini, "Achieving high data rate in multiband-OFDM UWB over power-line communication system," *IEEE Trans. Power Del.*, vol. 27, no. 3, pp. 1172–1177, Jul. 2012.

[3] S. Khedimallah, B. Nekhoul, K. Kerroum, and K. El Khamlichi Drissi, "Analysis of power line communications electromagnetic field in electrical networks taking into account the power transformers," in *Proc. IEEE Int. Symp. Electromagn. Compat.*, pp. 1–6, Sep. 2012, Rome, Italy.

[4] L. B. Wang, P. L. So, K. Y. See, M. Oswal, and T. S. Pang, "Investigation of radiated emissions in power line communication networks," in *Proc. IEEE Int. Power Eng. Conf. (IPEC 2007)*, pp. 455–460, Dec. 2007, Singapore.

[5] S. V. Tkachenko, R. Rambousky, and J. B. Nitsch, "Electromagnetic field coupling to a thin wire located symmetrically inside a rectangular enclosure," *IEEE Trans. Electromagn. Compat.*, vol. 55, no. 2, pp. 334–341, Apr. 2013.

[6] F. Rachidi, "A review of field-to-transmission line coupling models with special emphasis to lightning-induced voltages on overhead lines," *IEEE Trans. Electromagn. Compat.*, vol. 54, no. 4, pp. 898–911, Aug. 2012.

[7] C. A. Nucci, F. Rachidi, and M. Rubinstein, "Interaction of lightning-generated electromagnetic fields with overhead and underground cables," *The Lightning Electromagnetics*, pp. 687–718, Jan. 2012.

[8] A. Piantini and J. M. Janiszewski, "Lightning-induced voltages on overhead linesApplication of the extended rusck model," *IEEE Trans. Electromagn. Compat.*, vol. 51, no. 3, pp. 548–558, Aug. 2009.

[9] F. M. Tesche and T. Karlsson, *EMC Analysis Methods and Computational Models*, New York, USA:John Wiley & Sons, 1997.

[10] M. Ianoz, "Review of new developments in the modeling of lightning electromagnetic effects on overhead lines and buried cables," *IEEE Trans. Electromagn. Compat.*, vol. 49, no. 2, pp. 224–236, May 2007.

[11] G. E. Bridges, "Transient plane wave coupling to bare and insulated cables buried in a lossy half-space," *IEEE Trans. Electromagn. Compat.*, vol. 37, no. 1, pp. 62–70, Feb. 1995.

[12] E. Petrache, F. Rachidi, M. Paolone, C. A. Nucci, V. A. Rakov, and M. A. Uman, "Lightning induced disturbances in buried cables-part I: theory," *IEEE Trans. Electromagn. Compat.*, vol. 47, no. 3, pp. 498–508, Aug. 2005.

[13] M. Paolone, E. Petrache, F. Rachidi, C. Nucci, V. Rakov, M. Uman, D. Jordan, K. Rambo, J. Jerauld, M. Nyffeler *et al.*, "Lightning induced disturbances in buried cables-part II: experiment and model validation," *IEEE Trans. Electromagn. Compat.*, vol. 47, no. 3, pp. 509–520, Aug. 2005.

[14] C. R. Paul, "A comparison of the contributions of common-mode and differential-mode currents in radiated emissions," *IEEE Trans. Electromagn. Compat.*, vol. 31, no. 2, pp. 189–193, May 1989.

[15] D. Poljak, A. Shoory, F. Rachidi, S. Antonijevic, and S. V. Tkachenko, "Time-Domain generalized telegrapher's equations for the electromagnetic field coupling to finite length wires above a lossy ground," *IEEE Trans. Electromagn. Compat.*, vol. 54, no. 1, pp. 218–224, Feb. 2012.

[16] A. Vukicevic, F. Rachidi, M. Rubinstein, and S. V. Tkachenko, "On the evaluation of antenna-mode currents along transmission lines," *IEEE Trans. Electromagn. Compat.*, vol. 48, no. 4, pp. 693–700, Nov. 2006.

[17] A. Maffucci, G. Miano, and F. Villone, "An enhanced transmission line model for conducting wires," *IEEE Trans. Electromagn. Compat.*, vol. 46, no. 4, pp. 512–528, Nov. 2004.

[18] S. Chabane, P. Besnier, and M. Klingler, "Enhanced transmission line theory: Frequency-dependent line parameters and their insertion in a classical transmission line equation solver," in *Proc. IEEE Int. Symp. Electromagn. Compat.*, pp. 326–331, Aug. 2013, Denver, USA.

[19] F. Rachidi and S. Tkachenko, *Electromagnetic Field Interaction with Transmission Lines: From Classical Theory to HF Radiation Effects*. Southampton UK: WIT Press, 2008, vol. 5.

[20] D. Poljak, F. Rachidi, and S. V. Tkachenko, "Generalized form of telegrapher's equations for the electromagnetic field coupling to finite-length lines above a lossy ground," *IEEE Trans. Electromagn. Compat.*, vol. 49, no. 3, pp. 689–697, Aug. 2007.

[21] K. L. Kaiser, *Electromagnetic Compatibility Handbook*, CRC press, 2005.

[22] J. Nitsch and S. Tkachenko, "High-frequency multiconductor transmission-line theory," *Foundations of Physics*, vol. 40, no. 9-10, pp. 1231–1252, 2010.

[23] S. Wang and F. C. Lee, "Investigation of the transformation between differential-mode and common-mode noises in an EMI filter due to unbalance," *IEEE Trans. Electromagn. Compat.*, vol. 52, no. 3, pp. 578–587, 2010.

[24] S. Mikki and Y. Antar, "The antenna current greens function formalism: part I," *IEEE Trans. Ant. Prop.*, vol. 61, no. 9, pp. 4493–4504, Sep. 2013.

[25] C. R. Paul, *Analysis of Multiconductor Transmission Lines*. John Wiley & Sons, 2008.

[26] R. Rambousky, J. Nitsch, and H. Garbe, "Matching the termination of radiating non-uniform transmission-lines," *Advances in Radio Science*, vol. 11, no. 16, pp. 259–264, Jul. 2013.

[27] Y. Oguri, K. Murano, F. Xiao, and Y. Kami, "LCL characteristics of parallel transmission line with load circuit," in *Proc. Int. Symp. Electromagn. Compat.*, pp. 126–129, Oct. 2007, Qingdao, China.

[28] F. Grassi, X. Wu, Y. Yang, G. Spadacini, and S. A. Pignari, "Modeling of imbalance in differential lines targeted to spice simulation," *Prog. Electromagn. Research B*, vol. 62, pp. 225–239, Mar. 2015.

[29] S. J. Orfanidis, *Electromagnetic Waves and Antennas*. Rutgers University New Brunswick, NJ, 2002.

Mohammad Heggo (S'08) received his B.Sc. and M.Sc. degrees in Electrical Engineering from Ain Shams University, Cairo, Egypt, in 2006 and 2010, respectively. In 2007, he joined the research and development department, Elsewedy Electrometer Company, Egypt as an embedded communication software engineer. Since 2013, he is pursuing his Ph.D. degree in Electrical Engineering at the University of Liverpool, UK. In 2014, he was awarded a scholarship for two years from the Cognitive Communications Technology Department, Agency for Science, Technology, and Research, Singapore. His research interests include power line communication, electromagnetic interference to transmission lines, cognitive radio, MIMO communication systems and smart grid communications.

Xu Zhu (S'02 - M'03 - SM'12) received the B.Eng. degree (first class Hons.) from Huazhong University of Science and Technology, Wuhan, China, in 1999, and the Ph.D. degree from the Hong Kong University of Science and Technology, Hong Kong, in 2003. Since 2003, she has been an academic staff member of the Department of Electrical Engineering and Electronics, the University of Liverpool, Liverpool, U.K., where she is currently a Reader. She has over 140 peer-reviewed publications on communications and signal processing. Her research interests include MIMO, equalization, resource allocation, power line communication, cognitive radio and smart grid communication. She is an Editor for the IEEE Transactions on Wireless Communications, and has served as a Guest Editor for a number of international journals. She has served on a large number of conference organizing committees, e.g., as Symposium Chair of the IEEE ICC 2016.

Yi Huang (S'91 - M'96 - SM'06) received BSc in Physics (Wuhan University, China) in 1984, MSc (Eng) in Microwave Engineering (NRIET, Nanjing, China) in 1987, and DPhil in Communications from the University of Oxford, UK in 1994. He has been conducting research in wireless communications, applied electromagnetics, radar and antennas. His experience includes 3 years spent with NRIET (China) as a Radar Engineer and various periods with the Universities of Birmingham, Oxford, and Essex, UK. He worked as a Research Fellow at British Telecom Labs in 1994, and then joined the University of Liverpool, UK in 1995, where he is now a full Professor in Wireless Engineering, the Head of High Frequency Engineering Group and Deputy Head of Department. He has published over 300 refereed papers and is the principal author of Antennas: from Theory to Practice (John Wiley, 2008). He has received many research grants from research councils, government agencies, charity, EU and industry, acted as a consultant to various companies served on a number of national and international technical committees and been an Editor, Associate Editor or Guest Editor of four of international journals. He has been a keynote/invited speaker and organiser of many conferences and workshops (e.g. WiCom 2006, 2010, IEEE iWAT 2010, and LAPC2012). He is at present the Editor-in-Chief of Wireless Engineering and Technology, a UK National Rep of European COST-IC1102, Executive Committee Member of the IET Electromagnetics PN, a Senior Member of the IEEE, and a Fellow of the IET.

Sumei Sun is Head of the Cognitive Communications Technology Department, Institute for Infocomm Research, Agency for Science, Technology, and Research, Singapore. Her research focus is energy- and spectrum-efficient communication technologies for connecting human, machines, and things. Dr. Sun is inventor and co-inventor of thirty granted patents and more than thirty pending patent applications, many of which have been licensed to industry. She has authored and co-authored more than two hundred technical papers in prestigious IEEE journals and conferences. She has also been actively contributing to organizing conferences in different roles. Some of her recent conference services include Executive Vice Chair of Globecom 2017, Symposium Co-Chair of ICC 2015 and 2016, Track Co-Chair of IEEE VTC 2012 Spring, VTC 2014 Spring and VTC 2016 Fall, Publicity Co-Chair of PIMRC 2015, etc. She is an Editor for IEEE Transactions on Vehicular Technology (TVT) since 2011, Editor for IEEE Wireless Communication Letters during 2011-2016, and Editor of IEEE Communications Surveys and Tutorials since 2015. She received the "Top Editor Award" in 2016, "Top15 Outstanding Editors" recognition in 2014, and "Top Associate Editor" recognition in 2013 and 2012, all from TVT. She is a distinguished lecturer of IEEE Vehicular Technology Society 2014-2016, a co-recipient of the 16th PIMRC Best Paper Award, and Distinguished Visiting Fellow of the Royal Academy of Engineering, UK, in 2014. She is a Fellow of the IEEE, class 2016.